Book Chapter

Development of Antibacterial Additives: Biomaterials Based on Zeolites with Cu^{2+} and CuO Nanoparticles

Manuel F Meléndrez[1,9], Lina M Romero[1], Daniel A Palacio[2], Gabriela A Sánchez-Sanhueza[3], Eduardo Pérez-Tijerina[4], Francisco Solis-Pomar[4], C Montalba[5], Andres Jaramillo[6], Iván D Meléndrez[7] and Carlos Medina[8]*

[1]Interdisciplinary Group of Applied Nanotechnology (GINA), Hybrid Materials Laboratory (HML), Department of Materials Engineering (DIMAT), Faculty of Engineering, Universidad de Concepción, Chile
[2]Departamento de Polímeros, Facultad de Ciencias Químicas, Universidad de Concepción, Chile
[3]Department of Restorative Dentistry, Faculty of Dentistry, Universidad de Concepción, Chile
[4]Facultad de Ciencias Físico-Matemáticas, Universidad Autónoma de Nuevo León, San Nicolas de los Garza, Mexico
[5]Universidad de Talca, Departamento de Tecnologías Industriales, Chile
[6]Departamento de Ingeniería Mecánica, Universidad de Córdoba, Colombia
[7]Departamento de Ingeniería Industrial, Universidad de Córdoba, Colombia
[8]Department of Mechanical Engineering (DIM), Faculty of Engineering, Universidad de Concepción, Chile
[9]Unidad de Desarrollo Tecnológico, 2634 Av. Cordillera, Parque Industrial Coronel, Chile

***Corresponding Author:** Carlos Medina, Unidad de Desarrollo Tecnológico, 2634 Av. Cordillera, Parque Industrial Coronel, Box 4051, Concepcion 4191996, Chile, Tel.: + 4 12203187; Email: cmedinam@udec.cl

Published **October 12, 2023**

This Book Chapter is a republication of an article published by Carlos Medina, et al. at Nanomaterials in July 2023. (Romero, L.M.; Araya, N.; Palacio, D.A.; Sánchez-Sanhueza, G.A.; Pérez-Tijerina, E.; Solís, F.J.; Meléndrez, M.F.; Medina, C. Study of the Antibacterial Capacity of a Biomaterial of Zeolites Saturated with Copper Ions (Cu^{2+}) and Supported with Copper Oxide (CuO) Nanoparticles. Nanomaterials 2023, 13, 2140. https://doi.org/10.3390/nano13142140)

How to cite this book chapter: Manuel F Meléndrez, Lina M Romero, Daniel A Palacio, Gabriela A Sánchez-Sanhueza, Eduardo Pérez-Tijerina, Francisco Solis-Pomar, C Montalba, Andres Jaramillo, Iván D Meléndrez, Carlos Medina. Development of Antibacterial Additives: Biomaterials Based on Zeolites with Cu^{2+} and CuO Nanoparticles. In: Tenderwealth Clement Jackson, editor. Prime Archives in Nanotechnology. Hyderabad, India: Vide Leaf. 2023.

Author Contributions: Methodology and method validation, L. M. R. and G. S, formal analysis, N. A, E. P. and F. S, writing—original draft preparation, D. P, writing—review and editing, M. F. M, project administration and funding acquisition, C.M. All authors have read and agreed to the published version of the manuscript.

Data Availability Statement: The raw/processed data required to reproduce these findings cannot be shared at this time as the data are also part of an ongoing study.

Acknowledgments: The author thanks FONDEF Nº ID20I10040, FONDECYT Grants No (3220108and11201236), and to the Interdisciplinary Group of Advanced Nanocomposites (Grupo Interdisciplinario de Nanotecnología Aplicada, GINA-according its Spanish acronym) of the Department of Engineering Materials (DIMAT, according its Spanish acronym), Engineering School of the University of Concepción, for its

laboratory of nano spectroscopy (LAB-NANOSPECT). FONDEQUIP Project No EQM150139andValentina Lamilla and Juliana Meléndrez for their enormous support.

Conflicts of Interest: The authors declare no conflict of interest.

Abstract

In this work, copper (II) ions were saturated and copper oxide nanoparticles (CuO NPs) were supported in natural zeolite from Chile, by contacting the adsorbent material with copper ion precursor solution and mechanical agitation, respectively. The kinetic and physicochemical process of the adsorption of copper ions in the zeolite was studied, as well as the addition of CuO NPs, on the antibacterial properties. The results showed that the saturation of copper (II) ions in the zeolite is an efficient process, obtaining a concentration of copper ions of 27 g L^{-1} in a time of 30 minutes. The TEM images showed that a good dispersion of the CuO NPs was obtained by mechanical stirring. The material effectively inhibited the growth of gram-negative and gram-positive bacteria that have shown resistance to methicillin and carbapenem. Furthermore, the zeolite saturated with copper at the same concentration had a better bactericidal effect than the zeolite supported with CuO NPs. The results suggested that the ease of processing and low cost of copper (II) ion-saturated zeolitic material could potentially be used for dental biomedical applications, either directly or as a bactericidal additive for 3D printing filaments.

Keywords

Zeolites; Copper ions; Antibacterial; Nanoparticles

Introduction

Recently, minerals that present high porosity, such as zeolite, have represented a useful and economical alternative for the development of biomaterials with unique physical and chemical properties for numerous applications. The incorporation of metallic nanostructures with bactericidal properties can provide solutions in human medicine [1]. The diversity of applications is due, specifically, to the porosity of this material, which has a

structure with negatively charged cavities that make it a striking material due to the exchange of monovalent and divalent ions, the presence of hydroxyl groups and water molecules. [2]. Additionally, the lodging of other molecules in their cavities such as ammonia, nitrates [3].

Clinoptilotite type zeolites are one of the most abundant and important natural zeolites in the use of applications in human, veterinary medicine and environmental applications [4]. These are aluminosilicate minerals with tetrahedral anionic frameworks with well-defined channels and cavities, which can be occupied by water molecules or compensating cations. These neutralize the anionic charges in the cavities and in the formation of tetrahedral rings (Langella et al, 2000; Leung et al, 2007). Most types of zeolites are of volcanic origin and have the general formula $M_2/n:Al_2O_3:xSiO_2:yH_2O$, where M is the cation found in the cavities or pores of the material, knowing that the main structure is based on tetrahedrons. of AlO_4 and SiO_4 that share oxygen atoms between 1 to 3 atoms, so its variety of structure can vary as it extends in its three dimensions [5].

In the search for applications at the microbiological level, both organic and inorganic materials have been considered, such as clay materials [6], nanocellulose fibers, carbon nanotubes among other types of materials [7–10]. In this context, the use of Cu or CuO nanostructures have been highlighted as promising nanomaterials with high antibacterial capacity and great potential to be used against a wide variety of Gram-positive and Gram-negative bacteria [11-13], where the mechanism The action of bacteria is due to the reaction that these metals carry out when combined with the SH groups of enzymes that inactivate cellular proteins [14]. Lei et al. (2023), reported on KTO nanowires doped with Cu and Ag to enhance their biological activity, such as antibacterial properties. The nanomaterial developed solely with copper (1.0 Cu-KTO) obtained the same inhibition of the bacterial population as the nanomaterials doped with both metals, indicating the high bactericidal activity of copper and a new idea for the design and development of new antibacterial nanomaterials [15].

Rodríguez-Méndez et al, studied the formation of silver nanoparticles supported on a natural zeolite and evaluated its antimicrobial effect. The results showed that the nanoparticles were well dispersed and stable, and had a high bactericidal effect on large populations of bacteria [16]. Yao et al, Study the antimicrobial capacity of zeolites exchanged with Cu^{2+} and Zn^{2+} ions on *Escherichia coli* and *Staphylococcus aureus*, demonstrating that the cations of the respective metals were housed on the surfaces and cavities of the zeolites through the exchange processes ionic, as it was also demonstrated that saturated zeolites with Cu^{2+} ions show excellent antibacterial performance with *S. aureus* and reaching the mortalities of 100% with concentrations of Cu^{2+} 1000 mg L^{-1} after 1 h [17] . Cruces et al, studied the effect of bimetallic nanoparticles of copper/silver supported in geoaluminum materials such as antibacterial agents, finding a homogeneous distribution on the surface of the geomaterials and demonstrating that the use of geomaterials with nanoparticles supports increases the Contact surfaces of these, which is favored in a greater release of ions and directly improves the antibacterial activity, showing great advantage of the use of these aluminosilicate materials as antibacterial agents [11]. Chen et al, studied the ion release properties and their antibacterial efficiency of saturated zinc, copper and iron, observing a greater release of copper and zinc ions in the presence of a saline solution corresponding to 73% for zinc and 36% for copper and a minimum bactericidal concentration after 2 h of 32 μg mL^{-1} and 64 μg mL^{-1} for copper and zinc, respectively [19].

The objective of this research is focused on obtaining an antimicrobial biomaterial from a natural zeolite saturated with Cu^{2+} ions and supported with copper oxide nanoparticles, taking advantage of the high surface area of the zeolite that will allow the dispersion of CuO nanoparticles and the performance of antibacterial properties. Furthermore, natural zeolites have a great advantage due to their high availability, low cost, affinity for cation exchange, and non-toxic nature that makes them an efficient antimicrobial biomaterial. For this, concentrations of zeolites saturated with Cu^{2+} and CuO were evaluated, generating different discs and used as antibacterial biomaterial against

multi-resistant strains to antibiotics isolated in the dental biomedical field.

Materials and Methods

Reagents

Natural Zeolite (ZLn) (Zeomaule, Chile), hydrochloric acid (Sigma Aldrich, Chile), Pentahydrate copper sulfate ($CuSO_4 \cdot 5H_2O$, 99.8%) (Sigma Aldrich, Chile), Copper oxide (CuO) nanoparticles (US Research Nanomaterials Inc, EE.UU) , Ultrapure water. The reagents used in microbiological tests were selected based on the recommendations according to the Clinical and Laboratory Standard Institute (CLSI/M100-S30) [18] and modifications were made as described by Andrade et al, Vergara-Llanos et al. and Sacoto et al [20-22].

Zeolite Washing

Washing was performed out to eliminate all the residual and organic matter of the process of extraction of it and eliminate part of the presence of iron, using the procedure described by Valdés et al, 2012. In a round background flask, placed a ratio (1: 100), 1.0 g of ZLn per 100ml of hydrochloric acid (2.4 mol L^{-1}). The solution constantly remains 200 rpm for 24 h at room temperature. After 24 h washing with plenty of water is carried out to eliminate excess hydrochloric acid and centrifuge (> 9000 rpm) for10 min. The resulting sample was dried for 24 h to 65 °C [23].

Saturated Zeolite with Copper Ions

The saturation tests of the washed natural zeolite (ZLnL) evaluated the effect of three variables to achieve the greatest exchange capacity by the copper ions. For this, the exchange capacity was evaluated the zeolite content, the copper concentration, and the effect of contact time. To evaluate the different parameters, a certain quantity of zeolite was placed in contact with 15 mL of copper solution, from the pentahydrated copper sulfate salt ($CuSO_4 \cdot 5H2O$, 99.8%); the system was kept under constant stirring for 24 h at 200 rpm. i) The dose of zeolite

was varied (0.1, 0.25, 0.5, 0.75, 1.0 and 2.0 g) using a constant concentration of copper ions (50 g L^{-1}); ii) To evaluate the effect of copper concentrations, the zeolite dose was kept constant and the concentration of copper ions was varied (5.0, 10.0, 15.0, 20.0, 30.0, 40.0 and 50.0 g L^{-1}); iii) In the case of time variation, it was carried out at different contact times (0.5 h to 24.0 h) at a determined dose of zeolite and copper concentration. After each trial, the material obtained is centrifugal (> 10000 rpm) for 15 min and the solution is stored to be analyzed by atomic adsorption spectroscopy and to determine with the remaining copper contents. The saturated Zeolite is placed on a 60 ° C for 24 h and is passed through a mesh of (125μm), to be stored in hermetic containers for subsequent analysis and characterization. From now on, for clarity of the material obtained, the saturated zeolite (ZLnLCu) will be named.

Zeolite Supported with Copper Oxide Nanoparticles

The obtaining of nanoparticles supported on the surface of the zeolite was carried out by mechanical agitation that consisted of taking the previously ZLnLCu (27.0 g L^{-1}), and 63.0 g L^{-1} of nanoparticles added copper oxides (CuONPs) previously synthesized, size between 20-100 nm, to obtain a maximum concentration between copper ions and nanoparticles of 100.0 g L^{-1}. For this, the ZLnLCu was mixed with a certain amount of CuONPs sand homogenized with the help of an agate mortar until a homogeneous mixture was obtained. ZLnCu supported with CuONPs will be abbreviated as ZLnCuONPs.

Zeolite Characterization

The characterization of the ZLn, ZLnL, ZLnLCu, ZLnCuONPs were first performed by infrared spectroscopy (FTIR) with the attenuated total reflection function (ATR) (FTIR-ATR) using a spectrometer FTIR Spectrum Two (× 1720) (Perkin Elmer, Waltham, Ma, USA). The scanning Electronic Microscopy images (SEM) were performed using an electronic scanning microscope (JSM 6300 Ly model) with 20 kV acceleration voltage and the samples were also analyzed by X-ray spectroscopy of dispersive energy (EDS). Dee transmission

electronic microscopy images were performed using a JEM 1200 ex II Ex-transmission microscope (Jeol, Ltd, Tokyo, Japan) at a voltage of 120 kV. Selected area electron diffraction (SAED) was also carried in TEM in order to clarify the crystalline structure and to highlight further the presence of CuO particles in the composite product.

Microbiological Assays

In a first step antibacterial activity of all modificated zeolites against the clinical methicillin-resistant *Staphylococcus aureus* [24] strain and American Type Control Culture ATCC *Enterococcus faecalis* 29212 strain were performed by determination of Minimum Inhibitory Concentration (MIC) and Minimum Bactericidal Concentration (MBC). The strains were stored at -80 °C, were cultured for 18 to 24 h on Tryptic Soy Agar (TSA) plates at 37 °C. A colony was seeded into Tryptic Soy Broth (TSB) and incubated over night at 37 °C. The inoculum was adjusted to 0.5 Mc Farland (1.5-2 X 10^8 CFU mL^{-1}) using a turbidimeter, and then diluted 1/10 to reach $1X10^7$ CFU mL^{-1}. Preparation of 96 microwell plates was performed by the addition of 120 µL of Mueller-Hinton Broth (MHB) in each well.

The zeolite stock was prepared by mixing 250 mg in 5 mL of sterile water. By adding 120 µL of the stock in the first well with 120 µL of MHB, the concentration of well 1 (initial) was 7.81 mg mL^{-1}. From this, 10 dilutions were prepared.5 µL of the $1X10^7$ CFU mL^{-1} inoculum was added. This left a final inoculum of $5X10^5$ CFU mL^{-1}. Each microwell plate was incubated in at 37 °C for 24 h. After incubation, 10 µL of MTT (3-(4,5-dimethylthiazol-2-yl)-2,5-diphenyltretazole bromide) was added to each microwell. It was incubated for 30 min to visualize the color change, and then the MIC reading was done. Wells that turned purple were those showing bacterial growth (metabolically active bacteria). MTT is metabolically reduced because of the action of the electron transport chain. Non-viable bacteria or bacteria inhibited by an antibiotic will not induce the color change. 2 µl of each sample was inoculated in TSA and incubated for 48 h. The absence of growth implies a bactericidal

activity at that concentration. Additionally, to avoid *carry-over* possibilities, MBC determination was performed by filtering on 0.45-micron filter paper, washing with PBS and subsequent transfer to MHA according to CLSI recommendations (M26-A 2011). Subsequently, the growth at 24 and 48 h was observed.

In a second step, antibacterial activity of the modified zeolites against clinical methicillin-resistant strain *Staphylococcus aureus* [20] and carbapenem-resistant *Acinetobacter baummani* [21] strains were performed by agar diffusion assay. To do this, a series of discs was developed with the modified zeolites, to different concentrations, respectively. Discs were obtained using a brand and a mass due to 320 mg x-trip discs. This trial was repeated twice separately. Table 1 shows the different concentrations obtained between the different mixtures of the modified zeolites, to know the individual and synergistic effects of the antibacterial capacity of this biomaterial.

Table 1: Zeolite discs concentrations with the presence of copper ions and NPS for antimicrobial studies.

Tablets	**Copper concentration (mg L^{-1})**		
	ZLnLCu	**ZLnLCu+NPs**	**ZLnLNPs**
1	-	100000	63000
2	-	50000	50000
3	27000	27000	27000
4	10000	10000	10000
5	5000	5000	5000
6	1000	1000	1000

*In all the tests, a white tablet was made that corresponded to washed zeolite without NPs and copper ions.

Then, agar plates were prepared with 25 mL of MHA. The bacterial inoculum of each strain was prepared in the same way as for MIC until $1X10^7$ CFU mL^{-1}. A sterile torula was introduced into the inoculum until it was impregnated with the solution. A triplicate of each type of disc were exposed to UV light for 20 min per side and deposited on the agar, placed equidistant from each other and not less than 24 mm from center to center of the discs. With the plate closed, the tablets were

allowed to adhere to the agar for about 15 min and then incubated for 16-18 h at 37 °C. The plates were read after 16-18 h of incubation. The inhibition halos of the tablets were read with the back of the meter foot under reflected light.

Statistical Analysis

For antimicrobial assays, an ANOVA test with multiple comparisons (Tukey's method) was used, with 95% confidence intervals for calculating the differences. Differences were considered statistically significant at the 5% level. Data were analyzed using GraphPad Prism6.0 (GraphPad Inc, La Jolla, CA).

Results and Discussion

Characterizatation of ZLn and ZLnL

The chemical composition of ZLn was obtained by quantitative wave scattering X-ray fluorescence spectrometry (XRF) [25]. Through this analysis, the following compositional ranges were obtained (see Table 2): SiO_2 (63%-66%) and Al_2O_3 (10%-13%) as main components, in addition to appreciable amounts of Fe_2O_3 (1%-4%) and of CaO (2%-3%), less than Na_2O, K_2O, and MgO and only traces of MnO, TiO_2 and P_2O_5 were found. Finally, the percentage of moisture varied between 6 and 12%.

Table 2: Chemical composition and physical properties of the zeolite used.

Compounds	Composition %
SiO_2	64.19
TiO_2	0.51
Al_2O_3	11.65
Fe_2O_3	2.53
MnO	0.03
MgO	0.66
CaO	3.42
Na_2O	0.75

K_2O	1.60
Physical properties	
Cation exchange capacity (CIC)	86.82 a 112.88 cmol/Kg
Thermal stability	<450 ºC
Chemical stability (pH)	8.9
Main zeolitic component	Clinoptilolite-Mordenite.
Chemical name	Calcium potassium magnesium aluminosilicates hydrated

Once the washing was complete with the hydrochloric acid solution 2.4 mol L^{-1}, both the Natural and the washed zeolite were characterized by different techniques (FTIR-ATR and BET, SEM). Figure 1 shows the main characteristic bands attributed to zeolites, such as the presence of hydroxyl groups in the region of 3440 cm^{-1}, in the range between 2990 and 1600 cm^{-1} the presence of water molecules in the zeolite channels, 1005 cm^{-1} to the asymmetric vibrational modes of Si-O and Al-O bonds, main characteristics in the composition of the material and bands associated with the stretching vibrational modes of bonds between oxygen and elements such as silicon and aluminum.

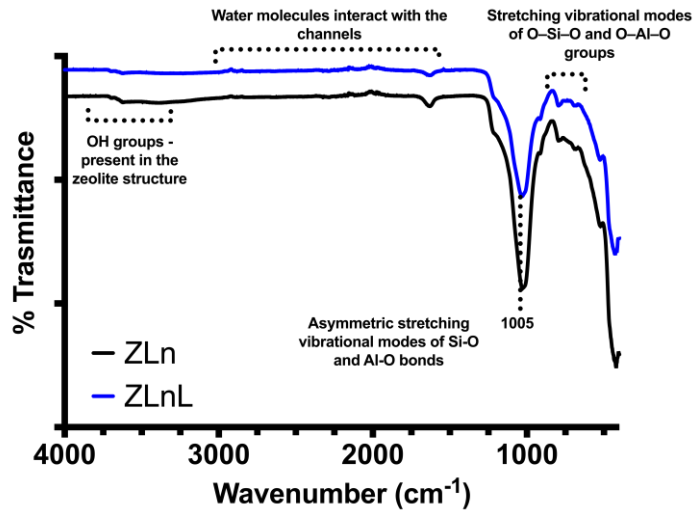

Figure 1: Characterization of Natural Zeolite (ZLn) before and after washing with hydrochloric acid (ZLnL) by FTIR.

Nitrogen gas adsorption tests at a temperature of 77 K were used to determine the specific surface area (Sg), pore volume (Vp), micropore volume (Vo), mesopore volume (Vm). Before each measurement, the degassing required for this type of analysis was carried out at a relatively low temperature (120 °C) for 3 h, which allows the elimination of water and possible adsorbed gases which could affect the analysis. Table 3 shows the N_2 adsorption-desorption isotherm values for natural zeolite (ZLn) and washed zeolite (ZLnL). The shape of the isotherms and the specific surface area (SBET) values obtained by the Brunauer-Emmett-Teller (BET) method and the pore volume (VP) calculated from the amount of nitrogen adsorbed at a relative pressure of 0.95 atm indicate which correspond to non-porous samples without the presence of micropores (see Figure S.1). However, it can be evidenced that the zeolite washing helped improve the specific surface area and at the same time increased the pore volume, this is due to the elimination of organic matter and impurities in the natural zeolite extraction process, in addition to eliminating large part of iron salts. These results are similar to those reported by Baghbanian et al, 2014, who used natural zeolite of the clinoptilolite type, which increased the surface area from 49.7 to 55.6 m^2 g^{-1} after acid washing [4].

Table 3: Determination of specific surface and pore volume.

Sample	**SBET m^2 g^{-1}**	**Pore volume cm^3 g^{-1}**
ZLn	36.2	0.044
ZLnL	58.6	0.054

Additionally, Natural and Washed Zeolites (ZLn and ZLnL) were morphologically characterized by scanning electron microscopy (SEM) and elemental analysis by energy dispersive X-ray spectroscopy (EDS). Figure 2A and 2B show the SEM images and EDS spectra of ZLn and ZLnL, respectively. The SEM images of the ZLn and ZLnL can be observed in which structurally considerable differences are not observed when washed with the acid solution, however, through EDS analysis, the main elements belonging to the zeolite-type structures are presented and they are correlated with what is reported in the

literature regarding the silicon-aluminum proportions of a Clinoptilolite-type zeolite [1,26], as the decrease in iron content in the biomaterial is also observed. Alternatively, through the values obtained by EDS, a slight decrease in the aluminum content present can be observed with reference to the natural zeolite, this decrease in the aluminum content is due to a decationization and dealuminization process [27].

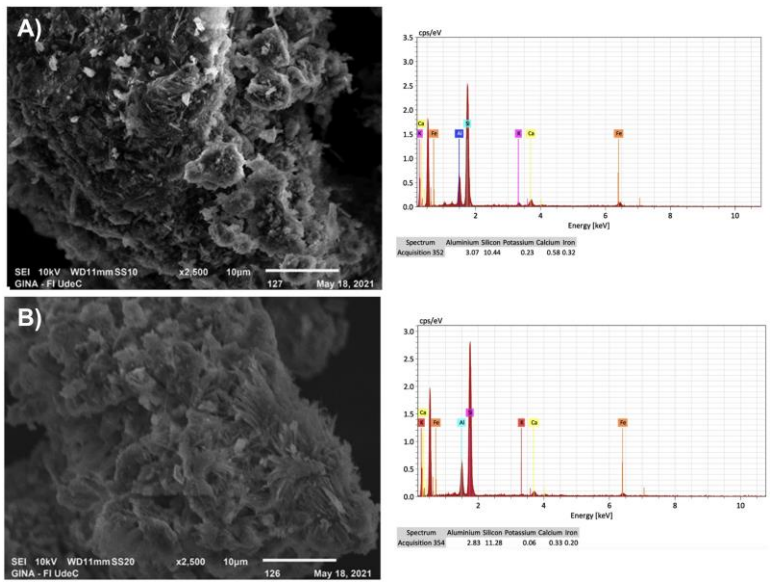

Figure 2: *SEM image and EDS spectrum of (a) ZLn and (b) ZLnL.*

Zeolite Saturation with Copper Ions

In Figure 3 (a), (b) and (c), the different adsorption studies of copper ions (II) in the zeolite are observed to determine the maximum ion retention capacity by means of cation exchange, to obtain a biomaterial with antimicrobial capacities, such as the use of natural Chilean zeolites saturated with copper ions and subsequently compatible with CuONP. In Figure 3a you can see the study of the variation of the effect of the zeolite, these studies are correlated as the dose increases if we observe the data in exchange percentages and this may be related to the increase in the surface area of the zeolite. However, for study purposes, the

saturation capacity was plotted, establishing the balance between the copper ions and the active sites of the zeolite, which shows a different trend as the content of zeolite in the material increases, and this may be explained by a superimposition of adsorption sites of the material [28].About saturation by varying the initial concentration of Copper, this being an important study since it helps us know the effective saturation capacity contained in the zeolitic material, in this case a constant dose of ZLnL (2.0 g) was used and it was varied the concentration of copper ions. Demonstrating that the saturation capacity of the zeolite increased with the increase in the concentration of copper ions, due to a phenomenon known as a concentration gradient, which causes that when increasing the concentrations, a force is exerted that overcomes the transfer of mass of the copper ions that are in solution and the active sites present in the ZLnL, these phenomena have been presented in studies where the removal of contaminants in carbonaceous materials has been reported [29]. With respect to the study of the variation of time (see figure 3c), it is an important factor to know the appropriate time where the greatest saturation is obtained and to reduce energy costs (economic) in the saturation processes and in a future escalation of the product, observing that maximum saturation is obtained at a time of 0.5 h and subsequently a slight desorption, due to the saturation of the active sites present in the zeolitic material. From this, it is concluded that the material has a copper concentration of 27,000 mg L^{-1}, using a dose of zeolitic material of 2.00 g dispersed in a solution of copper ions at a concentration of 50.0 g L^{-1} in 15 ml at 200 rpm for a period of 0.5 h and at room temperature.

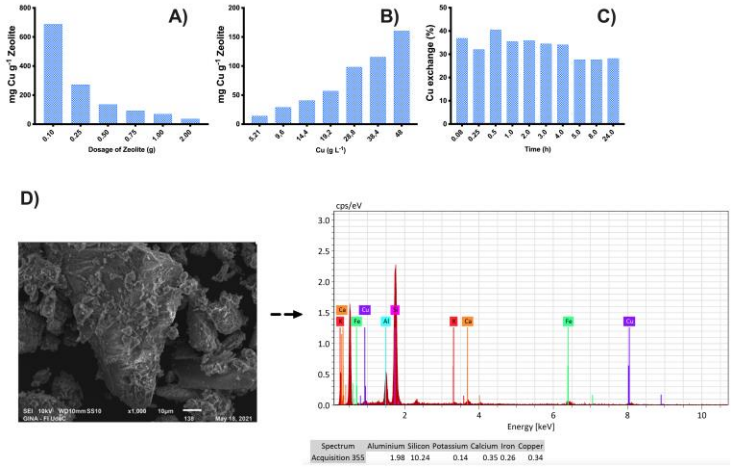

Figure 3: Study of the saturation capacity of zeolite with copper ions. (a) variation of the zeolite dose, (b) variation of the concentrations of copper ions, (c) study of the saturation capacity over time and (d) SEM image EDS spectrum Zeolite Saturated with Copper ions.

Figure S.2 shows the FTIR-ATR spectra of ZLnL compared with ZLnL in contact with different concentrations of Cu (ZLnLCu) at 10.0, 20.0, 30.0, and 50.0 g L^{-1}, representative of the saturation processes. Initially, the presence of symmetric and asymmetric stretching signals of the zeolitic material can be verified in 3325, 1620, 1052, 793, 556, 455 cm^{-1} characteristics of hydroxyl functional groups and vibrations of elements present in zeolitic materials of the clinoptilolite type [4,30]. While the ZLnL that are saturated with copper ions, as light shift of the O-H stretching band is observed, due to the Cu ion exchange process, with also the presence of slight attenuated bands around 1452 and 898 cm^{-1} attributed to exchange processes between sodium and copper ions [31-32]. These results are evidenced by SEM analysis that shows formation of copper salt layers in the ZLn particles in the exchange process and likewise verified by EDS analysis that shows copper content in the ZLn (see Figure 3d).

Copper Oxide Nanoparticles Supported on the Zeolite Surface

In Figure 4 shows the TEM images and the SAED pattern for the ZLnCuONPs samples, which confirmed that the copper oxide nanoparticles were supported on the surface of the ionically saturated zeolite, to provide a higher antimicrobial concentration to the zeolite biomaterial. The SAED pattern showed the continuous rings and was well separated from each other, where the rings were labeled as (starting from the inner ring): (1 1 0), (0 0 2), (1 1 1), (2 0 2), (0 2 0) and (0 2 2). The TEM and SAED results confirmed the successful support of the CuO nanoparticles [33-34]. The FTIR spectrum of ZLn and of ZLnCuONP is shown in Figure S.3. The FTIR spectra for the two samples have strong absorption bonds in the 3700 – 3300 cm^{-1} range which is due to the hydroxyl groups coordinated with the zeolite structure and corresponding to the water molecules. The vibrations within the lattice between 1300 and 450 cm^{-1} show slight changes in the main absorption peak of the zeolite, due to the presence of metal complexes or metal oxide nanoparticles. It can be observed that the spectrum of ZLnL (1080 cm^{-1}) compared to that of ZLnLCuONPs (1070 cm^{-1}) appears shifted, which may be due to the interaction of the zeolite network and the copper oxide nanoparticles. [35] Although the vibrational peaks of the CuO NPs are not highlighted, the presence of nanoparticles in the lattice and their interaction with the zeolite lattice has led to change all the particular peaks of the zeolite, especially the main range (1080 cm^{-1}), at lower wavelengths. On the other hand, the maximum intensity has been reduced in these areas [36].

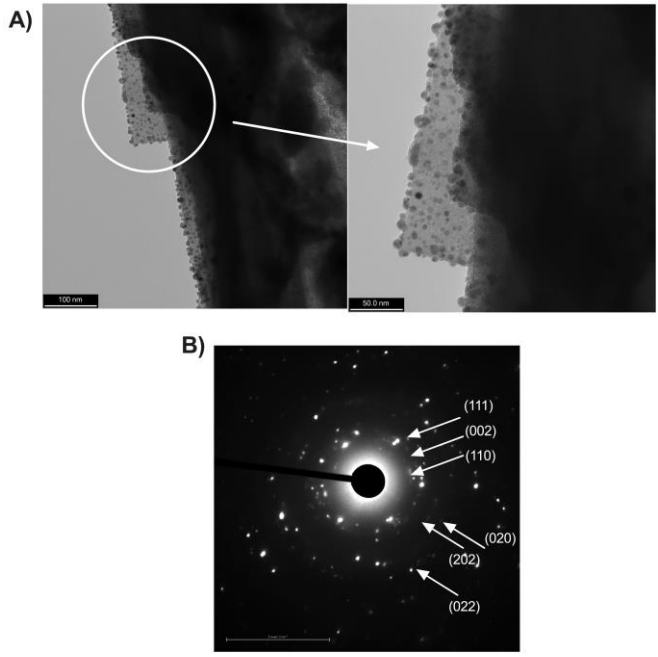

Figure 4: (A) TEM image and (B) corresponding SAED pattern of ZLnCuONPs.

Antibacterial Properties of the Biomaterial

The MIC of the zeolites tested against the clinical strain of S. aureus and the ATCC strain of *E. faecalis* were the same for ZLnL, with differences of at least 5 dilutions with respect to ZLnCu and ZLnCuONP. The results are presented in Table 4 and Figure 5. The results showed that in both strains, ZLnCu and ZLnCuONPs exhibited the same value for MBC. While, for *S. aureus*, the MIC was lower compared to *E. faecalis*.

Table 4: Mean values of minimum inhibitory concentration (MIC) and minimum bactericidal concentration (MBC) of modified zeolites through serial dilution test.

Bacterial Strain	**MIC (**mg mL^{-1}**) ± SD**			**MBC (**mg mL^{-1}**) ± SD**		
	ZLnL	ZLnCu	ZLnCuONPs	ZLnL	ZLnCu	ZLnCuONPs
E. faecalis ATCC 29212	7.8 ± 0.5	0.25 ± 0.05*	0.25 ± 0.01*	7.8 ± 0.5	1.12 ± 0.9*	3.9 ± 0.05
S. aureus UCO 99	7.8 ± 0.9	0.24 ± 0.01*	0.24 ± 0.02*	7.8 ± 0.9	1.12 ± 0.9*	3.9 ± 0.05

The values are represented as the average of triplicate MIC and MBC values and their respective standard deviation.
* Mean values with significant differences compared with ZLnL. ($P < 0.05$)

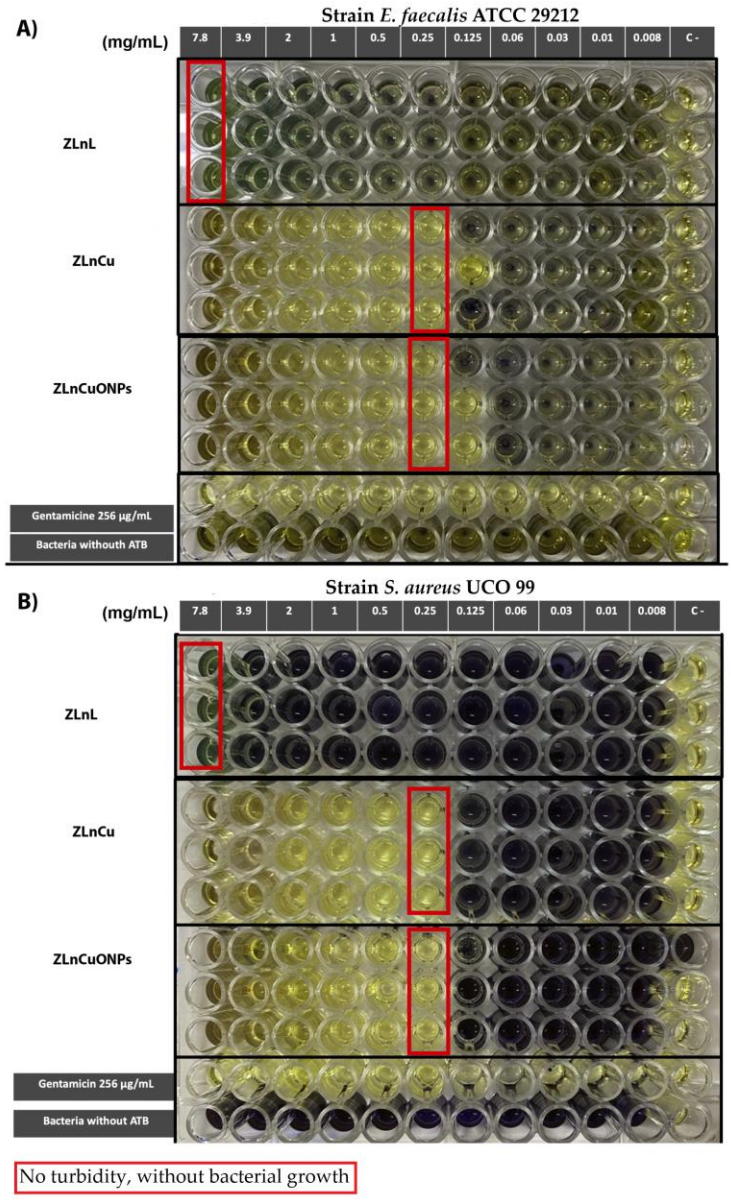

Figure 5: Broth dilution test: (a) MIC of Natural Zeolites and modified Zeolites against *E. faecalis*. (b) MIC of Natural Zeolites and modified Zeolites against *A. baumannii.*

Obtaining natural Chilean zeolite saturated with copper ions and its antibacterial activity has been previously described. Microbiological tests demonstrated that zeolite saturated with copper salt ions (ZLnCu) has antimicrobial activity with bactericidal effect against *Staphylococcus aureus* and ATCC *Enterococcus faecalis* 29212 strains, with a MIC of 0.24 and 0.25 mg mL^{-1}, respectively. This research has the advantage that, in addition to using a control strain, it demonstrates its antimicrobial activity against common multi-resistant clinical strains in the dental biomedical field [24,37]. The results show the bactericidal effect of the biomaterial and its potential application as a filler in dental materials. Vergara-Figueroa [38], reported the antibacterial activity of nanometer-sized zeolites doped with copper ions against methicillin-resistant *S. aureus*. The results suggested that the MIC of the antimicrobial used to inhibit bacterial growth was 0.75 mg mL^{-1}, which indicates that our biomaterial inhibits bacterial growth with two times less concentration than the one reported here. On the other hand, secondary endodontic infections show a high prevalence of *Enterococcus faecalis*, since they are capable of persisting after root canal treatment [38], so this biomaterial promises to be very useful in this field. Furthermore, little information has been found on zeolite with proven antibacterial properties with this bacterial strain. Malek et al. [39], studied the antibacterial activity of copper-exchanged Y zeolite synthesized from rice husk ash by disk diffusion technique. The results suggested that zeolite exchanged with 900 ppm copper has a bactericidal effect against *E. faecalis* with an inhibition halo of 2.25 mm. Although the results were obtained by different techniques, the effectiveness of the new ZLnCu material can be evidenced.

Zone of inhibition values were obtained for the different types of zeolites tested against the Gram-positive clinical strain *S. aureus* (Fig. 6a) and the Gram-negative clinical strain *A. baumannii* (Fig. 6b). The results are presented as mean values in Table 5. Both ZLnCu and ZLnCuONPs showed antibacterial activity against gram-negative and gram-positive bacteria. Although, ZLnCuONPs presented lower inhibition halos than ZLnCu, indicating that the addition of CuO nanoparticles does not affect the bactericidal activity of the material, but influences other points such as production cost.

Table 5: Average inhibition zone (mm) and standard deviation for modified zeolites through at different concentrations.

Bacterial strain	**ZLnCu Inhibition zone (mm)**				**ZLnCuONPs Inhibition zone (mm)**						**Control**	
	Concentrations (*g* L^{-1})										**ZLnL (-)**	**ATB** (+)
	1	**5**	**10**	**27**	**1**	**5**	**10**	**27**	**50**	**100**		
***S. aureus* UCO 99**	21.0±3.5 ^{B}	27.1±2.6 ^{A}	32.5±1.6* ^{A}	38.5±1.1* ^{A}	20.5±3.3 ^{B}	21.1±3.6 ^{B}	24.±3.2 ^{A}	28.8±2.9* ^{A}	32.6±1.5* ^{A}	36.8±0.7* ^{A}	19.5±2.9	21.0±0.3
***A. baumannii* UCO 538**	13.0±0.0 ^{C}	13.0±0.0 ^{C}	16.5±0.5 ^{C}	26.6±0.4* ^{A}	13.0±0.0 ^{C}	13.0±0.0 ^{C}	13.0±0.0 ^{C}	14.0±0.0 ^{C}	19.6±0.2 ^{C}	25.0±0.3*^{A}	13.0±0.0	21.0±0.3

Abbreviations: ZLnCu, cooper ions-saturated zeolite; ZLnCuONPs, Zeolite Supported with Copper Oxide Nanoparticles; ZLnL, washed natural zeolite. (A) Susceptible to antibacterial material. (B) Intermediate. (C) Not susceptible to antibacterial material

* Mean values with significant differences ($p < 0.05$)

In this study it was shown that ZLn do not have antimicrobial activity, and that the ZLnCu at the same concentration has better activity than the ZLnCuONPs for both the Gram-positive and Gram-negative strains, the Gram-positive bacteria being much more sensitive. This agrees with the results of Vergara-Figueroa [40] that classified as susceptible to an average of halos over 23 mm according to the CLSI [41]. The results presented in this study, carried out separately in two tests, each in triplicate, indicate, according to this cut-off point, that both *S. aureus* and *A. baumannii* tested are susceptible to saturated Zeolite from 27,000 mg mL^{-1}, that is, at 27 g mL^{-1} [40]. Similarly, the superior antibacterial efficacy of ZLnCu has also been reported to be due to the large surface area and small particle size of ZLnL[18].

Conclusions

From the results it was possible to determine the saturation capacity of the zeolite by adding copper ions and the mechanical support of copper oxide nanoparticles to evaluate its antibacterial activity. In the evaluation of the different experimental conditions, a copper ion saturation of 27.0 g L^{-1} could be achieved through an ion exchange process, verified by atomic adsorption and evidenced by EDS analysis. In addition, it was possible to demonstrate the support of the copper oxide nanoparticles on the surface of the zeolite with the TEM technique. With microbiological tests, it was possible to demonstrate that ion-modified copper zeolites/nanostructures can be useful as an antibacterial agent for dental biomedical applications. The toxicological aspects of these materials in future research will support these results.

References

1. Kraljević Pavelić S, Simović Medica J, Gumbarević D, Filošević A, Pržulj N, et al. Critical Review on Zeolite Clinoptilolite Safety and Medical Applications in Vivo. Front. Pharmacol. 2018; 9.
2. Çanli M, Abali Y. A Novel Turkish Natural Zeolite (Clinoptilolite) Treated with Hydrogen Peroxide for Ni^{2+}

Ions Removal from Aqueous Solutions. Desalination Water Treat. 2016; 57: 6925–6935.
3. Gaikwad RW, Warade AR. Removal of Nitrate from Groundwater by Using Natural Zeolite of Nizarneshwar Hills of Western India.J. Water Resour. Hydraul. Eng. 2014; 8.
4. Baghbanian SM, Yadollahy H, Tajbakhsh M, Farhang M, Biparva P. Palladium Nanoparticles Supported on Natural Nanozeolite Clinoptilolite as a Catalyst for Ligand and Copper-Free C–C and C–O Cross Coupling Reactions in Aqueous Medium. RSC Adv. 2014; 4: 62532–62543.
5. Bogdanov B, Georgiev D, Angelova K, Yaneva K. Natural Zeolites: Clinoptilolite Review. 2009; 7.
6. Jayrajsinh S, Shankar G, Agrawal YK, Bakre L. Montmorillonite Nanoclay asa Multifaceted Drug-Delivery Carrier: A Review. J. Drug Deliv. Sci. Technol. 2017; 39: 200–209.
7. de Faria AF, Perreault F, Shaulsky E, Arias Chavez LH, Elimelech M. Antimicrobial Electrospun Biopolymer Nanofiber Mats Functionalized with Graphene Oxide–Silver Nanocomposites. ACS Appl. Mater. Interfaces. 2015; 7: 12751–12759.
8. Moradpoor H, Safaei M, RezaMozaffari H, Sharifi R, Moslem Imani M, et al. An Overview of Recent Progress in Dental Applications of Zinc Oxide Nanoparticles. RSC Adv. 2021; 11: 21189–21206.
9. Perdikaki A, Galeou A, Pilatos G, Karatasios I, Kanellopoulos NK, et al. Ag and Cu Monometallic and Ag/Cu Bimetallic Nanoparticle–Graphene Composites with Enhanced Antibacterial Performance. ACS Appl. Mater. Interfaces. 2016; 8: 27498–27510.
10. Schiffman JD, Wang Y, Giannelis EP, Elimelech M. Biocidal Activity of Plasma Modified Electrospun Polysulfone Mats Functionalized with Polyethyleneimine-Capped Silver Nanoparticles. Langmuir. 2011; 27: 13159–13164.
11. Cruces E, Arancibia-Miranda N, Manquián-Cerda K, Perreault F, Bolan N, et al. Copper/Silver Bimetallic Nanoparticles Supported on Aluminosilicate Geomaterials as

Antibacterial Agents. ACS Appl. Nano Mater. 2022; 5: 1472–1483.
12. Ermini ML, Voliani V. Antimicrobial Nano-Agents: The Copper Age. ACS Nano. 2021; 15: 6008–6029.
13. Murthy HCA, Desalegn T, Kassa M, Abebe B, Assefa T. Synthesis of Green Copper Nanoparticles Using Medicinal Plant Hagenia Abyssinica (Brace) JF. Gmel. Leaf Extract: Antimicrobial Properties. J. Nanomater. 2020; 2020: e3924081.
14. Jeon HJ, Yi SC, Oh SG. Preparation and Antibacterial Effects of Ag–SiO2 Thin Films by Sol–Gel Method. Biomaterials. 2003; 24: 4921–4928.
15. Lei S, Qi Y, Zhao L, Shen Y, An H, et al. Synergistic Effect of Ag and Cu on Improving in Vitro Biological Properties of K2ti6o13 Nanowires for Potential Biomedical Applications. Social Science Research Network. 2022; 18.
16. Rodríguez-Méndez BG, López-Callejas R, Olguín MT, Valencia-Alvarado R, Mercado-Cabrera A, et al. Growth of Ag Particles from Ag-Zeolite by Pulsed Discharges in Water and Their Antibacterial Activity. Microporous Mesoporous Mater. 2017; 244: 235–243.
17. Yao G, Lei J, Zhang W, Yu C, Sun Z, et al. Antimicrobial Activity of X Zeolite Exchanged with Cu2+ and Zn2+ on Escherichia Coli and Staphylococcus Aureus. Environ. Sci. Pollut. Res. 2019; 26: 2782–2793.
18. Chen S, Popovich J, Zhang W, Ganser C, E Haydel, et al. Superior Ion Release Properties and Antibacterial Efficacy of Nanostructured Zeolites Ion-Exchanged with Zinc, Copper, and Iron. RSC Adv. 2018; 8: 37949–37957.
19. Ma W. Methods for Dilution Antimicrobial Susceptibility Tests for Bacteria That Grow Aerobically: Approved Standard. CLSI NCCLS2006,26, M7-A7.
20. Vergara-Llanos D, Koning T, Pavicic MF, Bello-Toledo H, Díaz-Gómez A, et al. Antibacterial and Cytotoxic Evaluation of Copper and Zinc Oxide Nanoparticles as a Potential Disinfectant Material of Connections in Implant Provisional Abutments: An in-Vitro Study. Arch. Oral Biol. 2021; 122: 105031.
21. Sacoto-Figueroa FK, Bello-Toledo HM, González-Rocha GE, Luengo Machuca L, Lima CA, et al. Molecular

Characterization and Antibacterial Activity of Oral Antibiotics and Copper Nanoparticles against Endodontic Pathogens Commonly Related to Health Care-Associated Infections. Clin. Oral Investig. 2021; 25: 6729–6741.
22. Andrade V, Martínez A, Rojas N, Bello-Toledo H, Flores P, et al. Antibacterial Activity against Streptococcus Mutans and Diametrical Tensile Strength of an Interim Cement Modified with Zinc Oxide Nanoparticles and Terpenes: An in Vitro Study. J. Prosthet. Dent. 2018; 119: 862.e1-862.e7.
23. Valdés H, Alejandro S, Zaror C. A. Natural Zeolite Reactivity towards Ozone: The Role of Compensating Cations. J. Hazard. Mater. 2012; 227–228: 34–40.
24. Quezada-Aguiluz M, Aguayo-Reyes A, Carrasco C, Mejías D, Saavedra P, et al. Phenotypic and Genotypic Characterization of Macrolide, Lincosamide and Streptogramin B Resistance among Clinical Methicillin-Resistant Staphylococcus Aureus Isolates in Chile. Antibiotics. 2022; 11: 1000.
25. ZeoMaule. (2021, 16 abril). Productos | ZeoMaule. ZeoMaule | Sitio Web Prototipo. Available online at: https://zeomaule.cl/productos/#:~:text=La%20zeolita%20es%20un%20fertilizante%20de%20liberaci%C3%B3n%20lenta,de%20agua%20y%20nutrientes%20disponible%20en%20la%20tierra.
26. Raiza AJ, Pandian K, Kumar RG. Biosynthesis of Copper Nanoparticles Supported on Zeolite Y and Its Application in Catalytic C-N Cross Coupling Reactions between Amines and Aryl Halides. Chemistry Select. 2019; 4: 1964–1970.
27. Rožić M, Cerjan-Stefanović Š, Kurajica S, Maěefat MR, Margeta K, et al. Decationization and Dealumination of Clinoptilolite Tuff and Ammonium Exchange on Acid-Modified Tuff. J. Colloid Interface Sci. 2005; 284: 48–56.
28. Shukla A, Zhang YH, Dubey P, Margrave JL, Shukla SS. The Role ofSawdust in the Removal of Unwanted Materials from Water. J. Hazard. Mater. 2002; 95: 137–152.
29. Pouretedal HR, Sadegh N. Effective Removal of Amoxicillin, Cephalexin, Tetracycline and Penicillin G from Aqueous Solutions Using Activated Carbon Nanoparticles Prepared from Vine Wood. J. Water Process Eng. 2014; 1: 64–73.

30. Harnos S, Onyestyák G, Kalló D. Cu and Cu2In Nanoparticles Supported on Amorphized Zeolites for the Selective Reduction of Biomass Derived Carboxylic Acids to Alcohols. Microporous Mesoporous Mater. 2013; 167: 109–116.
31. Ayodele OB. Rational Design of Zeolite Y Supported Oxalate and Borohydride Ligands Functionalized Cu Catalysts for CO2 Conversion to Specialty Chemicals. Appl. Catal. B Environ. 2022; 312: 121381.
32. Liu Y, Ren W, Cui H. Large-Scale Synthesis of Paratacamite Nanoparticles with Controlled Size and Morphology. Micro Amp Nano Lett. 2011; 6: 823–826.
33. Baroot AFA, Alheshibri M, Yamani ZH, Akhtar S, Kotb E, et al. A novel approach for fabrication ZnO/CuO nanocomposite via laser ablation in liquid and its antibacterial activity. Arabian Journal of Chemistry. 2021; 15: 103606.
34. Dey KK, Kumar A, Shanker R, Wan M, Yadav RR, et al. Growth morphologies, phase formation, optical & biological responses of nanostructures of CuO and their application as cooling fluid in high energy density devices. RSC Advances. 2012; 2: 1387-1403.
35. Razavi R, Loghman-Estarki MR. Synthesis and Characterizations of Copper Oxide Nanoparticles Within Zeolite Y. Journal of Cluster Science. 2012; 23: 1097-1106.
36. Alswat AA, Ahmad MB, Hussein MZ, Ibrahim NA, Saleh TA. Copper oxide nanoparticles-loaded zeolite and its characteristics and antibacterial activities. Journal of Materials Science & Technology. 2017; 33: 889-896.
37. Opazo-Capurro A, San Martín I, Quezada-Aguiluz M, Morales-León F, Domínguez-Yévenes M, et al. Evolutionary Dynamics of Carbapenem-Resistant Acinetobacter Baumannii Circulating in Chilean Hospitals. Infect. Genet. Evol. 2019; 73: 93–97.
38. Tennert C, Fuhrmann M, Wittmer A, Karygianni L, Altenburger MJ, et al. New Bacterial Composition in Primary and Persistent/Secondary Endodontic Infections with Respect to Clinical and Radiographic Findings. Journal of Endodontics. 2014; 40: 670-677.

39. Malek NANN, Azid NA, Hadi AA, Ishak SZ, Asraf MH, et al. Antibacterial activity of copper exchanged zeolite Y synthesized from rice husk ash. Malaysian Journal of Fundamental and Applied Sciences. 2018; 14: 450-453.
40. Vergara-Figueroa J, Alejandro-Martín S, Pesenti H, Cerda F, Fernández-Pérez A, et al. Obtaining Nanoparticles of Chilean Natural Zeolite and Its Ion Exchange with Copper Salt (Cu2+) for Antibacterial Applications. Materials. 2019; 12: 2202.
41. Humphries R, Bobenchik AM, Hindler JA, Schuetz AN. Overview of Changes to the Clinical and Laboratory Standards Institute Performance Standards for Antimicrobial Susceptibility Testing, M100, 31st Edition. J. Clin. Microbiol. 2021; 59: e00213-21.

Supplementary Materials

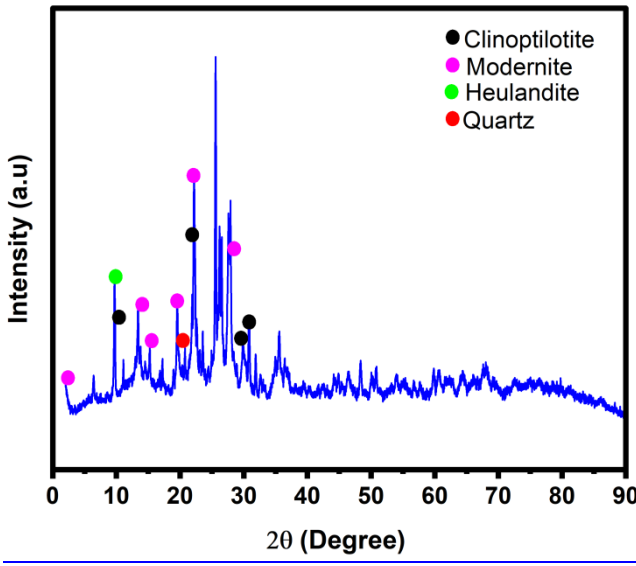

Figure S1: XRD pattern of natural zeolite (ZLn).

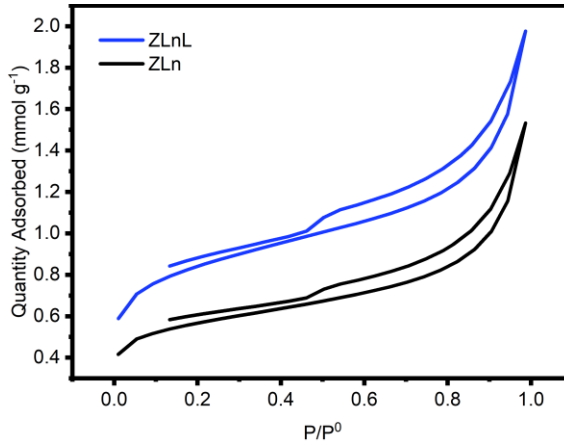

Figure S2: N_2 adsorption-desorption curve of ZLn and ZLnL.

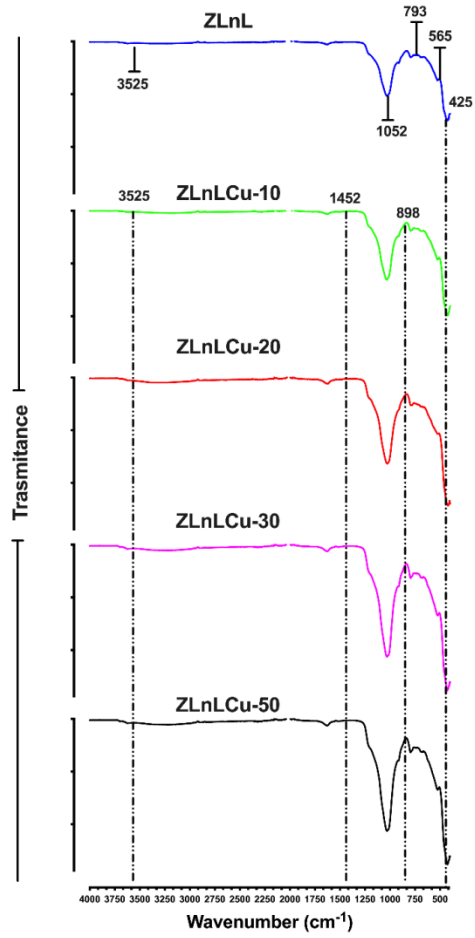

Figure S3: FTIR spectra of ZLnL before and after Cu^{2+} ion adsorption.

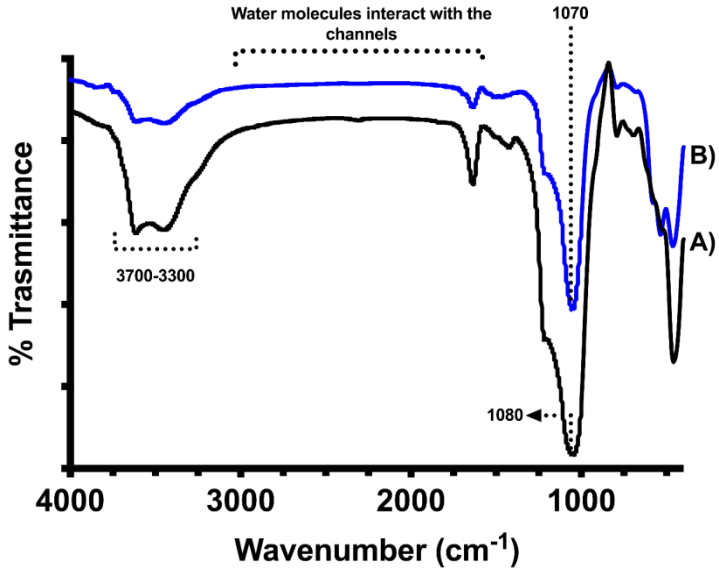

Figure S4: FTIR spectra of (A) ZLnL and (B) ZLnLCuONPS.